THE TRANSIENT BEHAVIOUR OF THE LONG WAVELENGTH CHANNEL OF ISOCAM

A. ABERGEL and M. A. MIVILLE-DESCHÊNES
Institut d'Astrophysique Spatiale, Université Paris-Sud, Bât. 121, 91405 Orsay, France

F. X. DÉSERT
Laboratoire d'Astrophysique Observatoire de Grenoble, BP 53, 414 rue de la piscine, 38041 Grenoble 9, France

M. PÉRAULT
Radioastronomie Millimétrique, Ecole Normale Supérieure, 24 rue Lhomond, 75005 Paris, France

H. AUSSEL and M. SAUVAGE
CEA, DSM/DAPNIA, CE-Saclay, 91191 Gif-sur-Yvette, France

(Received 17 June 1998; accepted 28 December 1998)

Abstract. The detector of the long wavelength channel of the ISOCAM camera on-board the Infrared Space Observatory is a Gallium doped Silicon photo-conductor hybridized by Indium bump. It presents systematic memory effects of the response which can bias the photometry by a factor of typically 40%. The main features of the response after flux variations are discussed. A simple empirical model actually used to correct systematically the data with a photometric accuracy of 5–10% is detailed.

Keywords: data processing, IR detectors, IR Imaging, ISO

1. Introduction

The ISOCAM camera is one of the four instruments on board the ISO satellite (Cesarsky *et al.*, 1996). It operates in the 2.5–18 μm range using two channels, the Short Wavelength one (SW) going from 2.5 to 5.5 μm, and the Long Wavelength one (LW) from 4 to 18 μm. The channels are selected using a wheel holding Fabry mirrors. The observing configuration is defined for each channel with a lens wheel to select the field of view per pixel (1.5, 3, 6 and 12″), and a filter wheel to select the spectral band pass. The filter wheel of the LW channel contains 10 broad band filters and two Continuously Variable Filters (CVF). The operating temperature of the camera in flight is around 3 K. This temperature is provided by liquid helium cooling. The detector used in the LW channel is a single crystal made of Gallium doped Silicon photo-conductor hybridized by Indium bumps. 32×32 square pixels are defined with a pitch of 100 μm. The crystal is 500 μm thick. The integration time allowed in flight are 0.28, 2, 5, 10 and 20 s.

A transient response after changes in photon flux levels is a well-known characteristics of extrinsic infrared photo-conductors working under low background

Experimental Astronomy **10:** 353–368, 2000.
© 2000 *Kluwer Academic Publishers. Printed in the Netherlands.*

conditions (see for instance Fouks and Schubert, 1995; Schubert *et al.*, 1995; Haegel *et al.*, 1996, and references therein). For each pixel of the LW channel of ISOCAM, the response after a flux variation is not instantaneous and strongly depends on what has been observed before. For most of the astronomical observations, the response is NEVER stabilised, and the photometry can be biased with a factor as high as 40%. However, for a given history of input flux starting from the switching on of the instrument, the response is always the same. Therefore, a correction of these effects is theoretically possible.

The prerequisite before developing any method of correction is a precise characterisation of the response at least for all configurations of the camera (and the illumination) used for all astronomical observations since the launch of ISO. A complete analysis of the whole ISOCAM database is still not achieved. The main features of the transient behaviour of the LW channel as it is actually understood are presented in Section 2. Both data obtained in orbit and during the ground-based calibration tests in the dedicated facility at the Institut d'Astrophysique Spatiale at Orsay, France (Pérault *et al.*, 1994) will be presented. Section 3 describes a method which can be systematically applied to most of the observations to correct the short-term transients with a precision of 5–10%. The limitations of this approach and future works are discussed in Section 4.

2. Description of the response after flux variations

2.1. Short-term and long-term transients

For most of the figures presented in this paper, we use the output units of the camera ('ADU': Analog to Digital Unit) divided by the electronic gain. On Figure 1 is presented an example of the response of the LW channel, going from the dark level to the zodiacal emission observed with the LW10 broad-band filter (8–15 μm and centered at 11.5 μm, coinciding to the 12 μm IRAS band). After an instantaneous jump of typically 60% of the total step, the signal looks stabilised after typically one minute (30 frames), but Figure 1b shows that a very long-term transient affects typically 5–10% of the flux above the dark level (Figure 1b). This transient can introduce a memory effect with an amplitude of a few % the input flux level, which can affect the data during several hours. In the following we consider that the response is made of a short-term transient and a long-term transient, with typical time constants equal to one minute and one hour respectively.

2.2. Characterisation of the short-term transients

The instantaneous jump to about 60% the total step of upward and downward short transients is a common feature for all pixels and all ground-based and in-flight observations. On the contrary the shape of the time variation for the remaining

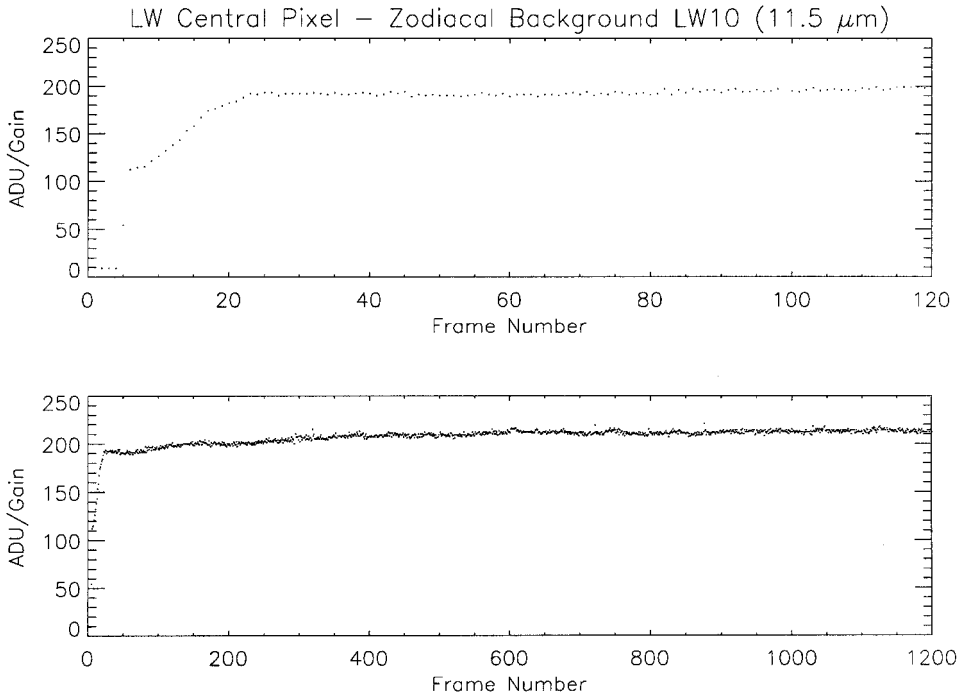

Figure 1. Response of the central pixel after a flux step going from the dark level to the zodiacal emission observed with the LW10 broad-band filter (8–15 μm and centered to 11.5 μm, coinciding to the 12 μm IRAS band). The integration time of each frame is 2.1 s. This observation was taken at the beginning of a revolution of ISO, just after the switching on of the camera. Upper panel: First frames showing the 'short-term transient' (see the text). Lower panel: Whole observation showing the 'long-term transient'.

40% after the instantaneous step strongly depends on:

- the flux history,
- the direction of the flux step (upward or downward),
- the signal detected before the flux step,
- the amplitude of the step,
- the pixel,
- the local spatial gradient of illumination.

A complete characterisation of the quantitative influence of the local spatial gradient of illumination to the response is not yet achieved. All results presented in this section concern uniform extended emission observed in orbit on the zodiacal background or during the ground-based tests.

The simplest response curves are obtained for small flux steps from levels significantly above the dark level (typically the zodiacal background observed with the broad-band filters). In such a case the upward and downward transients appear

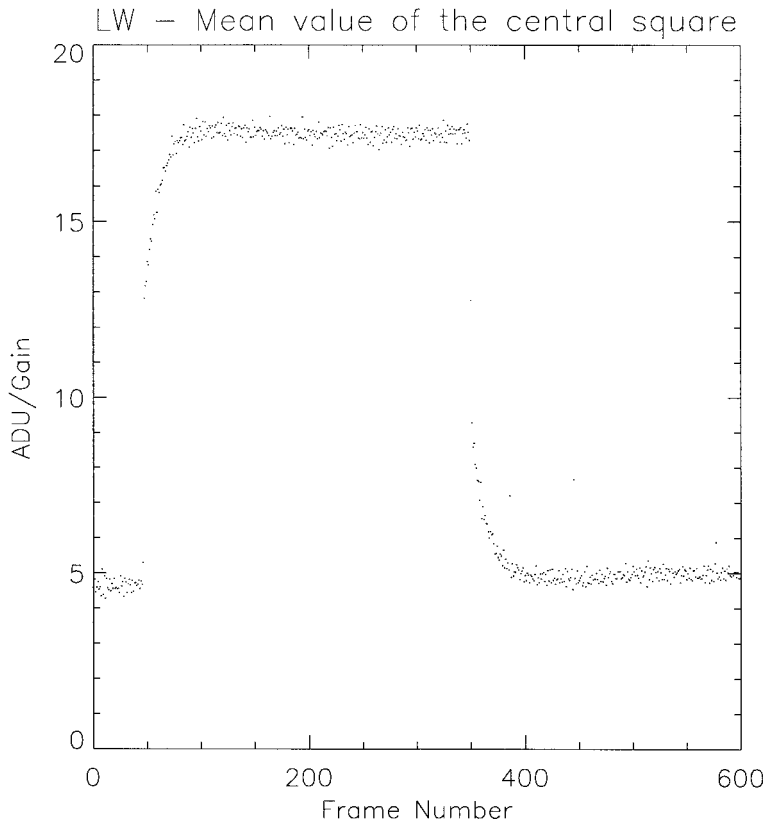

Figure 2. Example of upward and downward short transients for small steps starting from levels significantly above the dark level: Averaged response of the central 10×10 square obtained during the ground-based calibration tests. The integration time was 2.1 s.

symmetrical, and more or less exponential like for all pixels (Figure 2). Moreover the time constant decreases with the observed input flux. At the present time we have assumed that the time constant τ is inversely proportional to the input flux and identical for all pixels.

Going from the dark level or very low backgrounds (typically the zodiacal emission observed with a short wavelength position of the CVF) to a strong flux (typically the zodiacal emission observed with a broad band filter), the first readouts after the instantaneous jump present a slope lower than what is expected with an exponential curve (Figures 1a, 3 and 4). This slope depends on the pixel location on the detector (Figures 3 and 4), and for strong steps (strong extended background observed during the ground-based calibration tests and bright point sources observed in the sky) can be negative. Moreover, the transient curve may present an overshoot followed by oscillations, especially for bright point sources or extended bright regions with high spatial gradients (Figure 4). The overshoots and the oscillations are not actually fully characterised for all pixels. However, the fact

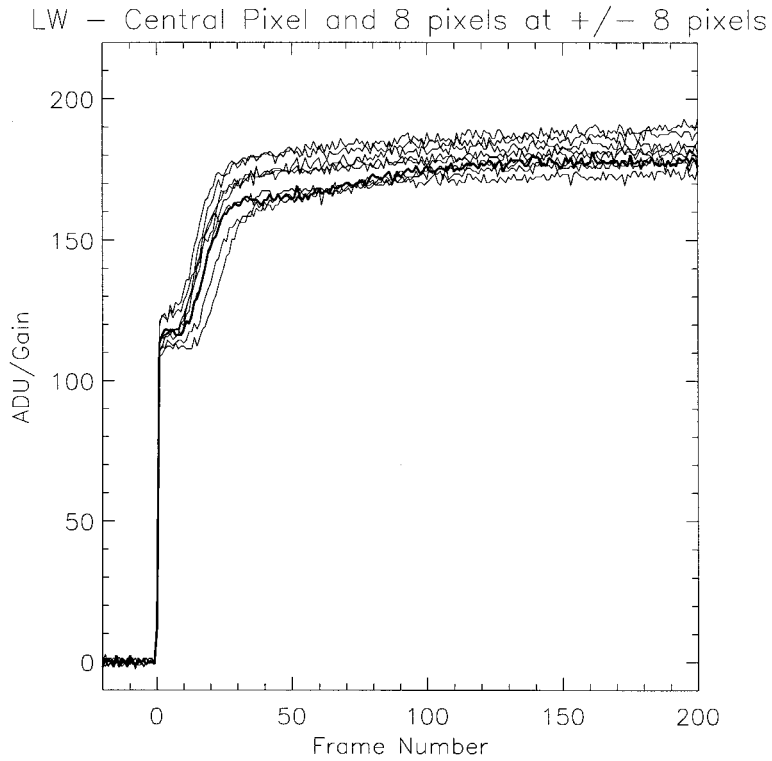

Figure 3. Example of strong upward short-term transients starting from the dark level for the central pixel (thick line) and for eight pixels located on a 16x16 square centered at the central pixel (the four corners and the four mid-points of the edges). Integration time: 2.1 s.

that such features are visible especially at the edge of the detector, where the local gradients of charges created inside the detector are high, indicates that these effects are mainly due to charge transfers.

Downward transients going to the dark level or low backgrounds are not symmetrical with upward transients (Figure 5), since they do not present any undershoot or bending point. Moreover, the decrease to the dark level is not exponential, and preliminary analysis indicate a decrease as t^{-n}, where t is the time since the change of flux and n is around 1 (Figure 5).

The response at time t depends on the tri-dimensional distribution of charges in the detector, thus is strongly dependent on the history of the input flux. An example is given on Figure 6. The more photons the pixels have received before time t, the quicker the response to a positive flux step at time t.

2.3. CHARACTERISATION OF THE LONG-TERM TRANSIENTS

A very long-term transient can affect typically 5–10% the flux above the dark level with a typical time constant of several hours, therefore a whole revolution

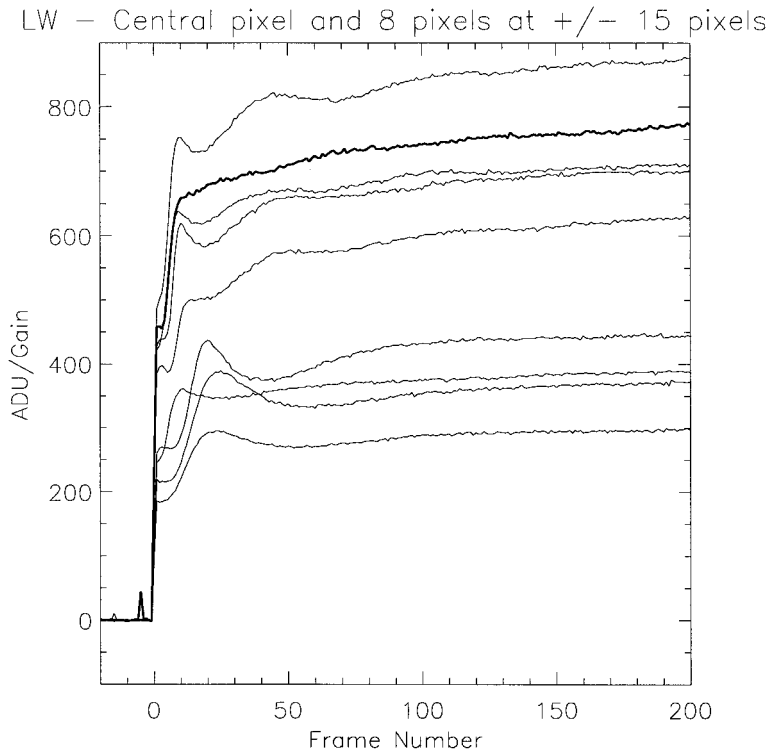

Figure 4. Example of very strong (ground-based data) upward short transients starting from the dark level, for the central pixel (thick line) and for eight pixels located at the four corners and the four mid-points edges of the detector (integration time: 2.1 s). Strong overshoots and oscillations are visible for all pixels at the edge of the detector where the spatial gradients of illumination are high. The response of the central pixel also present oscillations but with small amplitudes.

(Figure 1b). A complete characterisation of this effect is still to be achieved. This transient only affects the upward steps (compare Figures 1b and 5), and is extremely difficult to predict for one given observation since it strongly depends on what has been observed before. It is illustrated on Figure 7 which shows that the long-term transient is only detectable during the first observation of the orbit of the satellite.

3. Correction of the short-term transients

For most of the observations of the sky, the response of the pixels is NEVER stabilised. Without any correction, this memory effect biases the photometry with a factor which can be as high as 40%. However, the response for a given history of input flux starting from the switching on of the instrument is always the same. Therefore, a correction is theoretically possible.

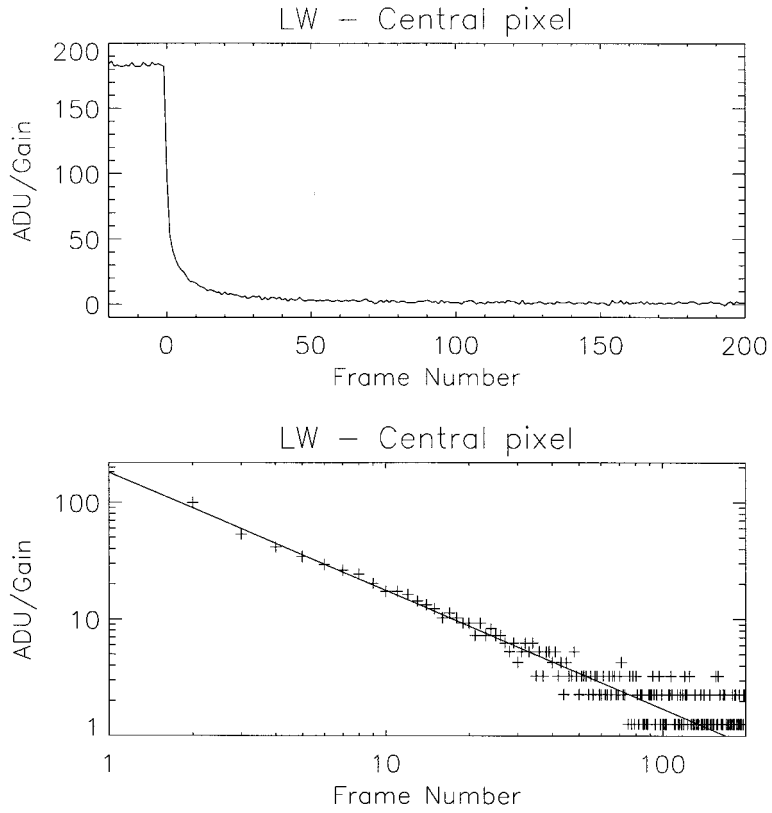

Figure 5. Upper panel: Example of downward transients to the dark level (ground-based data). Integration time: 2.1 s. Lower panel: The same with logarithmic scales. The continuous line corresponds to a t^{-1} decrease, t being the time since the change of flux.

If the number of readouts per sky position or spectral CVF position is large enough to show a significant fraction of the transient curve, it is possible to fit pixel per pixel the temporal response using a specific function to derive as well as possible a 'stabilised' value. However, for most of the observations, only an extremely limited part of the short-term transient curve is observed. In the general case, it is NOT possible to apply any fitting method to the data to correct the short-term transients.

Methods based on the inversion of a model of the response of the pixels are actually under development. The general principle is the following:

Let I be the successive input fluxes seen by one pixel, S the successive responses (I and S are in units of *ADU Gain*$^{-1}$ s^{-1}). If the cross-talk between pixels is neglected, a direct model of the response measured by the pixel can be theoretically represented using a mathematical functional 'M' so that S = M(I). Obviously M may depend on I or S, and on the history of all the trend parameters of the system. An ideal transient correction consists to define an inverse model 'M^{-1}' and then

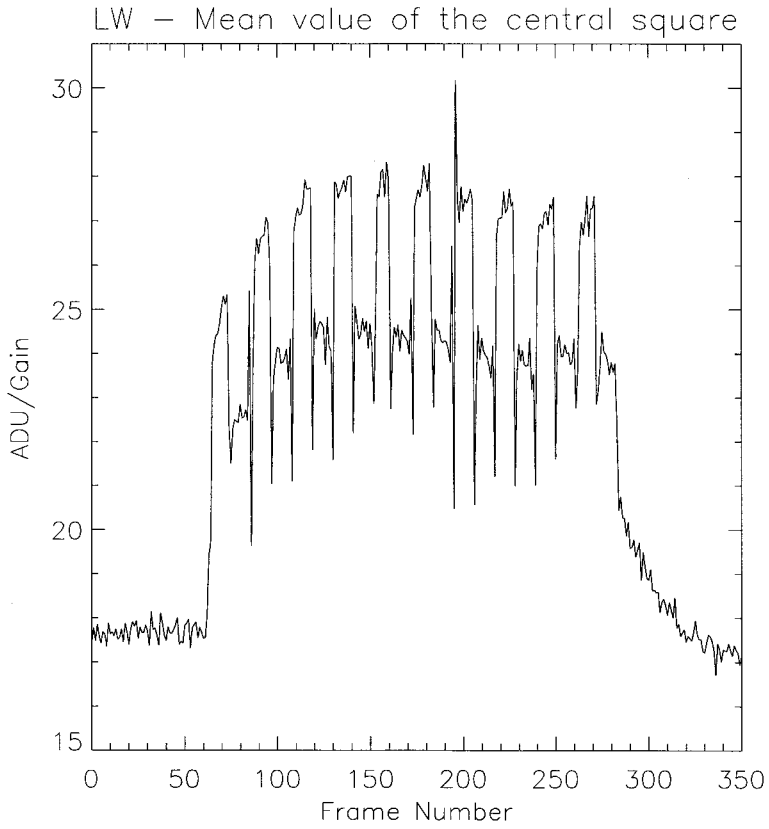

Figure 6. Dependence of the flux history on the response: an example for the short-term transient. This observation was taken during the Performance Verification phase of ISO. The zodiacal background was observed ('empty field'), and the input flux modulated by moving the filter wheel at three different positions. The measured signal quickly decreases at all changes of flux because of the rotation of the filter wheel.

to compute $I = M^{-1}(S)$. M may be purely empirical and/or based on physical considerations. The more precise your direct model (M), the better the correction. The problem is first to estimate M, then to inverse it.

We present in the next two sub-sections an empirical method used during the last two years to analyse systematically all the data of the LW channel of ISOCAM. It has been initially developed by Abergel *et al*. (1996) to correct the data obtained during observations in a raster mode of the extended dust emission in dense molecular clouds.

3.1. A SIMPLIFIED MODEL OF THE RESPONSE

A purely empirical model has been developed to reproduce the simplest cases of short-term transients (see Section 2.2) which correspond to limited flux steps from levels significantly above the dark level (typically the zodiacal background

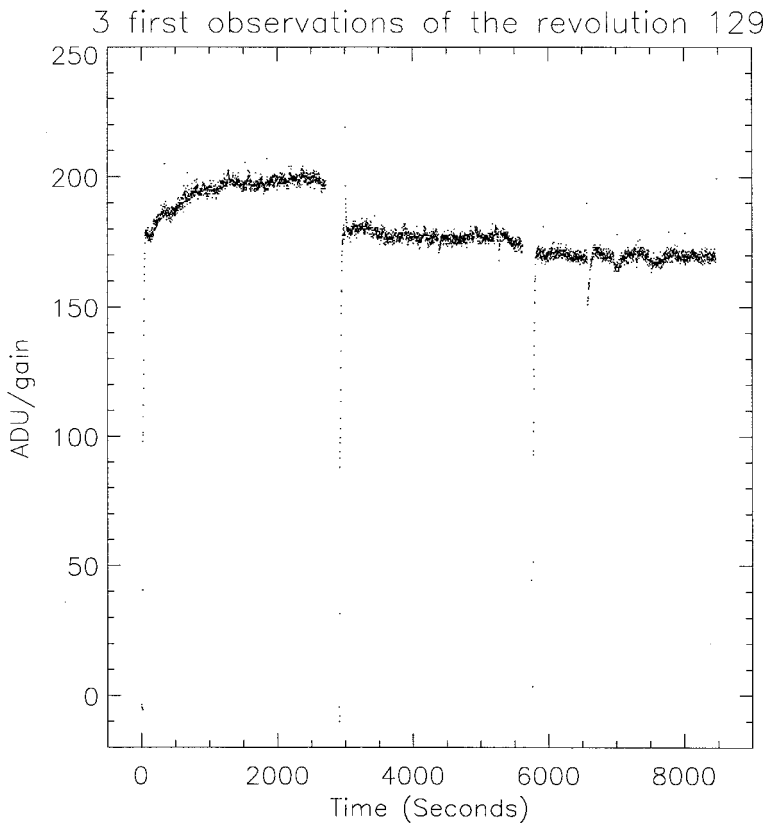

Figure 7. Evolution of the central pixel during the the three first observations of the revolution 129, corresponding to three pointings at different positions of the zodiacal background with the LW10 broad-band filter (12–18 μm centered at 11.5 μm). The integration time is 2.1 s. Only the first observation seems affected by the long-term upward transient.

observed with the broad-band filters). In this case, we have seen that the upward and downward transients are symmetrical, and more or less exponential-like for all pixels (Figure 2). The cross talk between pixels is neglected.

The response $s(t)$ of one given pixel as a function of the input flux $i(t)$ is given with the formula ($i(t)$ and $s(t)$ are in units of *ADU Gain*$^{-1}$ s^{-1}):

$$s(t) = ri(t) + (1 - r) \int_{-\infty}^{t} i(t') \frac{e^{-\frac{t-t'}{\tau}}}{\tau} dt' \tag{1}$$

The time constant τ in the integral depends on the time t′, since it is inversely proportional to the input flux:

$$\tau = \frac{\alpha}{i(t')} \tag{2}$$

It is easy to verify that, for a step of flux going from i_1 to i_2, this formula gives an instantaneous response equal to to $r \times (i_2 - i_1)$, followed by an exponential variation for the remaining $(1 - r) \times (i_2 - i_1)$, with two time constants inversely proportional to i_1 and i_2.

From preliminary fitting of the model with the transient responses recorded during a dedicated orbit (revolution 16, during the Performance Verification phase, where cycles of filter sequences were performed), the values of r and α have been adjusted to $r = 0.6$ and α = 1200 *ADU Gain*$^{-1}$.

The signal to noise ratio and the fact that the model is extremely simplified have not allowed to detect any significant variations of these values between pixels, though these are likely to occur.

Practically, the camera is not read continuously but rather we obtain a discrete series of readouts for all t_j. Thus we can rewrite Equation (2) in this way:

$$S(t_i) = r\,I(t_i) + (1 - r) \sum_{j=-\infty}^{i-1} \int_{t_j}^{t_{j+1}} I(t_j) \frac{e^{-(\frac{t_i - t'}{\tau_j})}}{\tau_j} dt' \tag{3}$$

With $\tau_j = \alpha / I(t_j)$.

During an integration, it is assumed (1) that one given pixel sees the same point in the sky and (2) that the configuration of the instrument is constant. The effects due to the jitter during the integration and to commanded changes of the pointing which may occur during an integration are neglected. Thus $I(t)$ is assumed constant between t_j and t_{j+1} and the integral of Equation (3) can be computed for all the terms in the summation. It comes:

$$S(t_i) = r\,I(t_i) + (1 - r) \sum_{j=-\infty}^{i-1} I(t_j) e^{\frac{t_j - t_i}{\tau_j}} (e^{\frac{t_{j+1} - t_j}{\tau_j}} - 1) \tag{4}$$

This simplified model allows to reproduce the response after a step of flux with a precision of typically 5–10%. It fails especially:

- For large flux steps (higher than typically 80 *ADU Gain*$^{-1}$ s^{-1}) since upward transients are not exponential-like because of the slope just after the instantaneous jump (see Figure 3) and unpredicted oscillations,
- For downward transients to a very low level (as for instance observed with a CVF on the zodiacal background) or to the dark, since the response curve is described more precisely by an hyperbolic curve rather than with an exponential curve (Figure 5).

3.2. INVERSION OF THE SIMPLIFIED MODEL OF THE RESPONSE

The transient correction consists in computing the successive values of $I(t_j)$ from the successive CAM readouts $S(t_j)$. It is important to note that r and α are fixed parameters of the model: this method does not use any fitting and can be applied whatever the state of the camera and the flux step are. The idea is to invert the Equation (4), which can easily be done with the two following assumptions:

1. We do not know the values of CAM readouts $S(t_j)$ from $t = -\infty$, since the time series is in the general case cut at the beginning of each observation (at $t = t_0$). It is thus necessary to assume a realistic history of the input flux before the first readout of the observation to proceed further. For all the illustrating tests presented in this paper (Figures 8 and 9), we have assumed that a constant input flux has been observed from $t = -\infty$ up to $t = t_0$, which means that the camera was assumed to be stabilized before the first readout. This translates in starting our summation at $j = 0$ and adding to Equation (4) a constant C_i.

2. In Equation (4), for the different values of j, we have $\tau_j = \alpha / I(t_j)$. The successive values of τ_j are not known since they depend on the successive $I(t_j)$. Thus, to allow a simple inversion of Equation (4), we have assumed that $\tau_j = \alpha / S(t_j)$. This assumption obviously leads to inappropriate corrections since, because of the transient effect, S and I can be much different. A detailed assessment of the impact of this approximation on the photometric accuracy is yet to be made. An alternative approach would consist first to consider that $\tau_j = \alpha / S(t_j)$ and compute an estimate of the successive values of $I(t_j)$, and then to iterate.

Practically speaking, if our observation is made of N readouts obtained at time $t_0, t_1, \ldots, t_{N-1}$, we can rewrite for each pixel Equation (4) in a matricial form:

$$S = [M] \times I + C \ .$$

S is the vector of N readouts, i.e. the data, I is the vector of N intensities, i.e the data corrected for transients.

$[M]$ is an N × N transfer matrix whose elements $M_{i,j}$ are such that:

- if $j > i$, then $M_{i,j} = 0$,
- if $j = i$, then $M_{i,j} = r$,
- if $j < i$, then $M_{i,j} = (1 - r) e^{\frac{t_j - t_i}{\tau_j}} (e^{\frac{t_{j+1} - t_j}{\tau_j}} - 1)$.

C is is a vector of constants as explained in assumption (1). For a constant input flux $I(t_0)$ observed from $t = -\infty$ up to the first readout (at $t = t_0$), we have for all

i, $C_i = (1 - r) \times I(t_0) \times e^{\frac{t_0 - t_i}{\tau_0}}$, with $\tau_0 = \alpha / I(t_0)$.

Finally, for all instants t_i, we have: $S(t_i) = \sum_{j=0}^{N-1} M_{i,j} \times I(t_j) + C_i$.

The transient correction consists in computing $I = [M]^{-1} \times (S - C)$. This is always possible since the determinant of the matrix [M] is never equal to zero (all elements of the main diagonal are equal to r, while the elements above the main diagonal are equal to 0). If the correction is perfect, the vector I represents the successive values measured by a detector with no memory effect.

3.3. EXAMPLES AND LIMITATIONS

Figure 8 shows an example of transient corrections for upward and downward transients from the zodiacal background to the emission of molecular clouds. Various levels of flux that were blurred due to transients in the original data, because the satellite spent a limited time at each position, become obvious on the corrected data, even for small flux steps. However, the model adopted to describe the response is obviously over-simplified and fails for strong flux steps, for downward transients to very low levels and for pixels with high gradient of illumination, especially point sources. This is illustrated for strong flux steps on Figure 9 where we show data coming from two pixels that see the brightest region of an observation of Centaurus A in the LW3 filter (12–18 μm) and with the 3″ pixel field of view lens. In the upper panel a strong step occurs and as a result, the corrected data (thick line) show an overshoot for the upward transient and an undershoot for the downward transient. This effect is much reduced in the lower panel where the maximum flux steps are 1/2 those in the upper panel.

4. Conclusions

The simple method we have presented allows a correction of short-term transients, without any parameter adjustment. The correction is limited in precision by the precision of the model of the response we use which is obviously oversimplified. It fails especially:

1. For downward and upward strong steps, since the model is symmetrical while the response is not,
2. For downward transients to the dark levels since the model assumes exponential-like decrease of the signal while the decreases appear rather hyperbolic,
3. For pixels with high gradient of illumination (especially point sources) since the model neglects the charge coupling.

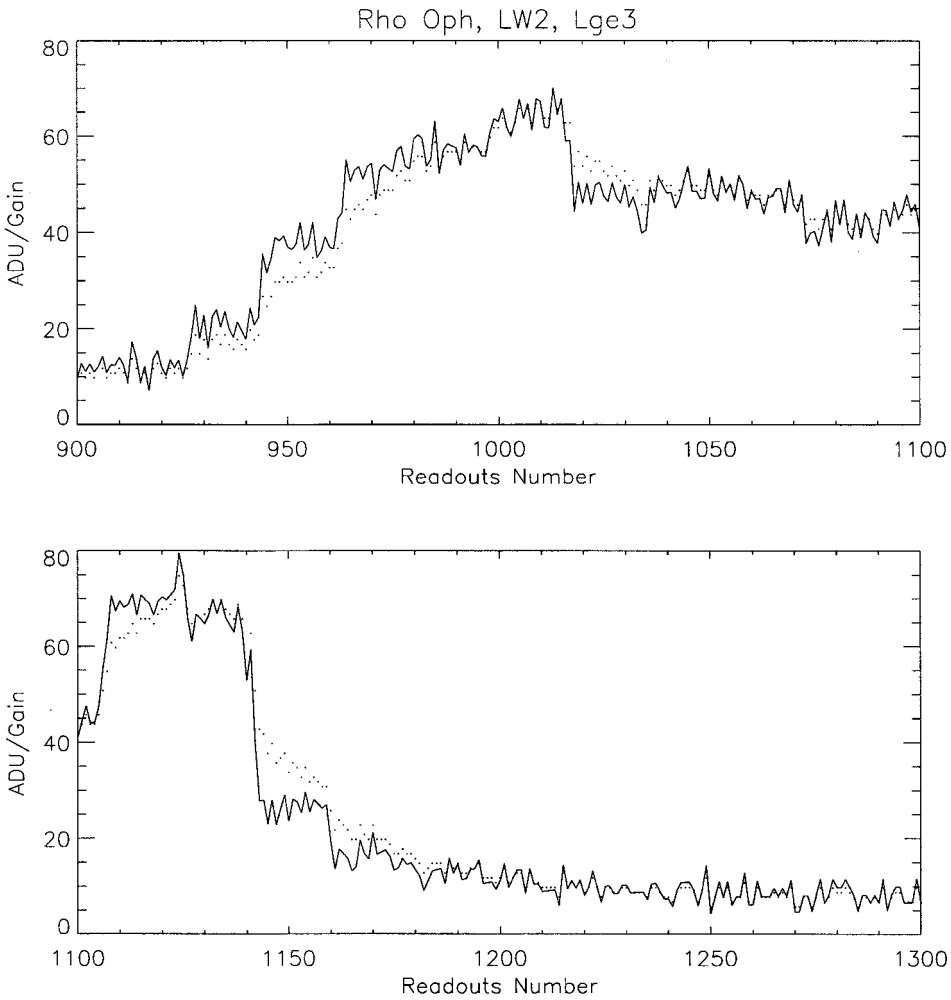

Figure 8. Example of transient correction on diffuse emission, taken from the observations of the main cloud of ρ Oph (Abergel *et al*., 1996) made with the LW2 filter (5–8.5 μm) and with a 3″ pixel field of view lens.
Dots: non corrected observation.
Solid line: transient corrected observation.
Upper panel: a typical time series from the zodiacal background to the diffuse emission of molecular clouds.
Lower panel: a typical time series from the diffuse emission of molecular clouds to the zodiacal background.

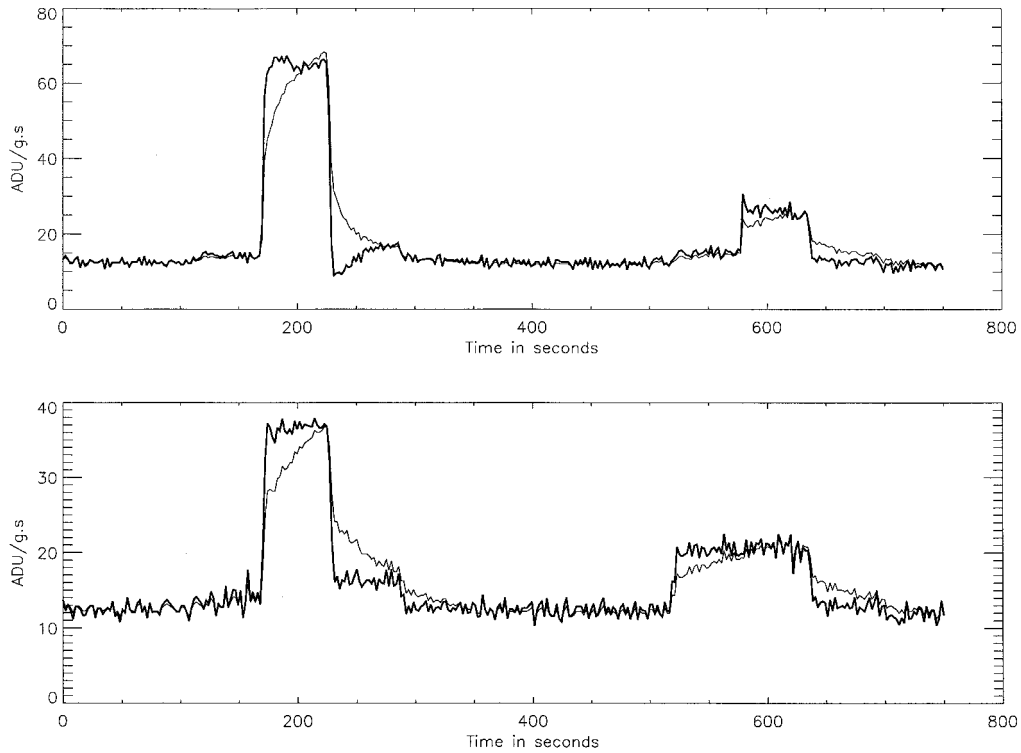

Figure 9. Pixel response in *ADU Gain*$^{-1}$ s^{-1} versus time during an observation on Centaurus A using the LW3 filter (12–18 μm) and the 3″ pixel field of view lens. In both cases the thin line is the original data, while the thick line is the transient corrected data. The upper panel shows how the formula used to described the transient behavior of the detector fails on strong steps: it creates an overshoot and undershoot for upward and downward steps respectively. In the lower panel, where the flux steps are smaller (the y axis scale is half that of the upper panel) the overshoots and undershoots are gone and the correction is much cleaner.

The model can be 'manually' adjusted, by using several time constants in the formula of the direct model defined by Equation (1), or by modifying its general expression. For instance we have checked that the following equation:

$$s(t) = ri(t) + (1-r)\int_{-\infty}^{t} i(t')\left(\frac{t-t'}{\tau} + a\right)\frac{e^{-\frac{t-t'}{\tau}}}{\tau}dt' \tag{5}$$

generally gives an remarkable fit for the first part of most of upward transients (not the oscillations). The slope just after the instantaneous jump is adjusted with the parameter a. However the value of a is generally not constant for all observations, and the corrections of downward transients are not improved since the Equation (5) is still symmetrical. This model fails in the general case, and can only be used to correct the observations dominated by a strong upward short-term transient.

Coulais and Abergel (1999) have recently presented a new approach based on the analytical inversion of the model of Fouks and Schubert (1995) (see also Schubert et al., 1995) developed for the PHT-S detectors of ISOPHOT. The first results for extended emission are extremely promising, since the accuracy of the correction appears $\sim$1% while the computing time is decreased by more than 10. Systematic tests are curently performed in order to be able to correct systematically the data in a pipe-line. However the Fouks and Schubert model fails to reproduce the oscillations after strong upward steps which are believed to be due to charge coupling. Finally, the long-term transient which may affect typically 5–10% the flux above the dark level with typical time scales of several hours still has to be fully caracterized by analysing data over whole orbits. Actually, only observations which are made with a significant spectral or spatial redundancy over a large time scale can be corrected from long-term transients (Miville-Deschênes et al., 1999).

At the present time there is no systematic method to correct data in a pipe-line to produce results with a photometric uncertainty better than 5 to 10%, but recent developements are promising. Paradoxically, the precision is NOT better for strong sources than for faint sources because of the not proper correction of the transient response. The unique sensitivity of the long wavelength channel of ISOCAM is still not fully used.

Acknowledgments

We thank the different teams at IAS, CEA-Saclay and ESA for their outstanding work and continuous support during all phases of the ISO project.

References

Abergel, A. *et al.*: 1996, ISOCAM mapping of the ρ Ophiuchi main cloud, A&A 315, L329.

Cesarsky, C. J. *et al*.: 1996, 'ISOCAM in flight', A&A **315**, L32.
Coulais, A. and Abergel, A.: 1999, 'Transient correction of the ISOCAM data with the Fouks-Schubert model: First results', The Universe as seen by ISO, Proc ESA SP-427.
Fouks, B. I. and Schubert, J.: 1995, 'Precise theoretical description of the photoresponse for detectors of ISOPHOT's Si:Ga array', Proc. SPIE 2475 487.
Haegel, N. M., Newton, C., Simoes, J. C. and White, A. M.: 1996, 'Modeling of the transient response in far infrared photoconductors', Proc. 30th ESLAB Symp. Submillimeter and Far-Infrared Space Instrumentation, ESA SP-388, 15–20.
Miville-Deschênes et al.: 1999, in preparation.
Pérault, M., Désert, F. X. and Abergel, A. *et al*., 1994, *Opt. Engineering* **33**, 762.
Schubert, J., Fouks, B. I., Lemke, D. and Wolf, J.: 1995, 'Transient Response of ISOPHOT Si:Ga Infrared Photodetectors: Experimental results and Application of the Theory of nonstationary processes', Proc. SPIE 2553 461.